Advanced Midcourse Guidance for Air-to-Air Missiles

V.H.L. Cheng* and N.K. Gupta†
Integrated Systems, Inc., Palo Alto, California

This paper considers the midcourse guidance of beyond-visual-range air-to-air tactical missiles where seeker lock-on is not achieved at launch. An advanced midcourse guidance law is derived based on an optimal-control formulation. The midcourse guidance formulation minimizes flight time subject to a terminal intercept condition. The optimality conditions of the control problem result in a two-point boundary-value problem, which is too complex for real-time onboard implementation with near-term computer technology. This paper applies singular perturbation techniques and engineering approximations to completely eliminate the need for solving two-point boundary-value problems. The resulting advanced guidance law is near-optimal and sufficiently simple for implementation. Computer simulations are used to compare the performance of this advanced guidance law to those of an existing linear-optimal guidance and a proportional navigation guidance, which are both modified with vertical *g*-bias commands prescribed by the sponsoring agency for midcourse trajectory shaping. The advanced guidance law developed in this paper shows substantial improvement over the other two guidance laws through expanded outer launch boundaries.

I. Introduction

PREVIOUS studies have developed advanced guidance laws for short range air-to-air missiles using modern control methods. Potential improvements in missile capability are impressive.[1,2] Advances in very large scale integration (VLSI) and very high speed integrated circuit (VHSIC) technologies are likely to make these guidance laws cost effective to implement. This paper studies guidance logic for the midcourse phase of beyond-visual-range (BVR) missiles where requirements differ significantly from those of the terminal phase.

In medium and long-range missiles, seeker lock-on is not feasible or desirable at launch; consequently, the missile depends on target position and velocity updates from the launch aircraft. The generic BVR missile considered here can perform effectively, under the most favorable conditions, at launch ranges up to about 160 km (100 miles). The midcourse phase of the flight is defined as the period following launch until seeker lock-on is realized. Tactical considerations, including launch aircraft vulnerability, dictate short flight time as the basic performance index (which is the same as maximizing F-pole). In addition, missile energy must be conserved during the midcourse phase so that sufficient energy is available for terminal engagement of intelligent targets.

Conventional air-to-air missiles use proportional navigation (pronav) guidance or some of its modifications.[3-7] A preprogrammed vertical *g*-bias command is used to conserve energy in the midcourse phase by flying the missile at higher altitudes. Guidance laws based on optimal control theory can improve performance significantly.

In this paper, we develop an advanced midcourse guidance law based on a minimum flight-time optimal control formulation. Specifically, the optimal control problem is considered at each guidance cycle of the guidance computer, with the updated missile and target states. The resulting guidance command is used until the next guidance cycle when new state information is available. This dependence of the guidance command on available state constitutes a feedback guidance law, which allows the missile to adapt to unanticipated changes in the target state. The ultimate objective is to obtain a guidance algorithm suitable for real-time implementation onboard the missile with available microprocessor technology.

A straightforward solution of the optimal-control problem leads to a two-point boundary-value problem[8] (TPBVP), which is too complex for real-time onboard implementation. A typical TPBVP solver would involve iterations of forward integration of the state equations and backward integration of the adjoint equations until the solution converges. Singular perturbation techniques are used to simplify the optimal control problem. The resulting near-optimal control problem does not require the solution of any TPBVP. Similar time-range optimal control problems have been studied for aircraft applications in which thrust magnitude control is available, most notably by Kelley[9] and Calise et al.[10,11]

The formulation and development of the midcourse guidance law are contained in Sec. II. Section III compares the performance of the guidance law with two other conventional guidance laws, based on computer simulation results. Section IV is a summary of the paper.

II. Guidance Algorithm Development

This section shows a beyond-visual-range (BVR) missile model and describes the advanced midcourse guidance law based on an optimal control formulation and singular perturbation techniques.

Seeker measurements are not available during the midcourse flight to provide target information. For such information, the medium-range missile has to depend on periodic updates supplied by the launch aircraft or other tracking platforms. To enhance intercept performance against maneuvering targets, the missile guidance is repeated at each sample instant, using the latest available information about the target and missile states. This completes the midcourse guidance and control loop. Since the set of all possible target maneuvers during the midcourse period can lead to vastly different trajectories, the missile's dependence on in-flight target update to adapt its own trajectory in a feedback manner is crucial for consistent performance. This reduces the need to make, at best, unjustified assumptions on the target's future maneuver tactics. In the formulation, it is assumed that the missile is

Received Aug. 26, 1983; revison received June 11, 1985.

*Senior Research Scientist. Member AIAA.
†President. Member AIAA.

launched at time $t=0$. At sample instant $t=t_0\geq 0$, the problem with initial time t_0 and a free but optimal terminal time t_f is studied. Observe that the optimal terminal time t_f, corresponding to different initial time t_0, may be different, leading to a real-time feedback guidance law.

A. Missile Model

The missile model is based on a set of state variables that can be conveniently partitioned through time-scale separation for the particular mission we are concerned with. The state variables are 1) the missile position coordinates x, y, and h in a Cartesian inertial frame, where h represents altitude; 2) the specific energy $E:=h+V^2/2g$, where V denotes the total missile speed; and 3) the flight path angle γ and heading angle ϕ (see Fig. 1). The state equations are

$$\dot{x}=V\cos\gamma\cos\phi, \qquad x(t_0)=x_0 \tag{1}$$

$$\dot{y}=V\cos\gamma\sin\phi, \qquad y(t_0)=y_0 \tag{2}$$

$$\dot{h}=V\sin\gamma, \qquad h(t_0)=h_0 \tag{3}$$

$$\dot{E}=(T-D)V/(mg), \qquad E(t_0)=E_0 \tag{4}$$

$$\dot{\phi}=L\sin\sigma/(mV\cos\gamma), \qquad \phi(t_0)=\phi_0 \tag{5}$$

$$\dot{\gamma}=(L\cos\sigma-mg\cos\gamma)/(mV) \qquad \gamma(t_0)=\gamma_0 \tag{6}$$

The input control to be optimized is a lift vector in the two-dimensional subspace normal to the missile velocity vector, defined by magnitude L and orientation σ. The thrust T and mass m time-histories are predefined functions of time, and the thrust component normal to the velocity vector is ignored. The drag is defined by the usual quadratic dependence on angle of attack

$$D=QsC_D \tag{7}$$

where

$$C_D=C_{D_0}+C_{D_\alpha}|\alpha|+C_{D_{\alpha^2}}\alpha^2 \tag{8}$$

$$Q=\tfrac{1}{2}\rho(h)V^2 \tag{9}$$

α is the total angle-of-attack and the air density ρ is a function of altitude. The total angle-of-attack is related to lift magnitude L as follows

$$L=QsC_{L_\alpha}\alpha \tag{10}$$

Observe that the drag definition of Eq. (7) is used only in the guidance development formulation, while a more realistic calculation is used in the simulation software for performance analysis.

The target state is not considered directly in the state equations. The in-flight available target state is instead used to predict a point of intercept by the resulting algorithm presented in Sec. II E. This predicted intercept point is treated as a terminal condition for the system of Eqs. (1-6), and a minimum flight-time solution is sought. It is readily observed that using the predicted point of intercept as a terminal condition is only a matter of convenience and simplification, as the target may not arrive at that point in space exactly at the same time as the minimum flight-time solution. Consequently, any reasonable method of prediction can be used. For this study, the intercept point as predicted during midcourse is based on a constant-velocity target and a constant-speed missile. Note further that the time associated with the point of intercept prediction is not used by the formulation. The terminal condition can thus be identified as

$$(x,y,h)(t_f)=(x_f,y_f,h_f) \tag{11}$$

B. Optimal Control Formulation

For the sake of simplicity, the performance index is selected here as the time of flight: Minimize

$$J=\int_{t_0}^{t_f} dt \tag{12}$$

where the final terminal time t_f is a free parameter. A more general performance index can also be used here. The optimal control problem is to solve for the control variables that minimize J in Eq. (12), subject to the differential constraints of Eqs. (1-6) and the terminal condition of Eq. (11). The control variables are

1) $L:[t_0,t_f]\rightarrow R_+$, the commanded missile lift, which is assumed to be equal to the actual lift since the autopilot has a much faster time constant than the missile state dynamics.

2) σ: $[t_0,t_f]\rightarrow]-\pi,\pi]$, the lift orientation.

The solution to the optimal-control problem can be obtained by defining a Hamiltonian as follows

$$H=\lambda_\xi^T\xi+1 \tag{13}$$

where $\xi:=(x,y,h,E,\phi,\gamma)^T$, and $\lambda_\xi:=(\lambda_x,\lambda_y,\lambda_h,\lambda_E,\lambda_\phi,\lambda_\gamma)^T$ are the corresponding Lagrange multipliers. The Lagrange variables satisfy

$$\dot{\lambda}_\xi=-(\partial H/\partial\xi)^T, \quad \lambda_\xi(t_f)=(\nu_x,\nu_y,\nu_h,0,0,0)^T \tag{14}$$

Observe that λ_x and λ_y are constants since H does not depend explicitly on x and y. The optimality conditions are

$$\partial H/\partial L=0, \qquad \partial H/\partial\sigma=0, \qquad H(t_f)=0$$

where the last equation is the transversality condition due to the free final time. Note that H is an explicit function of time

Table 1 Typical midcourse parameter values for BVR missiles

$r=100{,}000$ m	
$h_{\max}=20{,}000$ m	
$V=1{,}000$ ms^{-1}	
$s=0.024$ m^2	
$m_0=135$ kg	
$L_{\max}=40$ mg	
$T=33{,}000$ N,	$0\leq t\leq 1.5$
$=7{,}500$ N,	$1.5\leq t\leq 8.5$
$=0$ N	$8{,}5\leq t$
$\dot{m}=-14.53$ kgs^{-1},	$0\leq t\leq 1.5$
$=3.31$ kgs^{-1},	$1.5\leq t\leq 8.5$
$=0$,	$8.5\leq t$

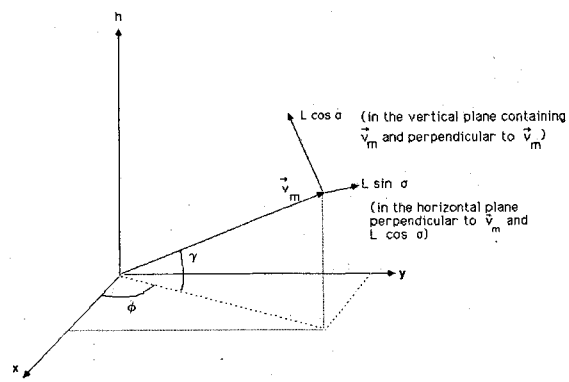

Fig. 1 Axis system for missile dynamics.

through thrust T and mass m; therefore, H is not constant (i.e., not equal to zero throughout).

The resulting TPBVP includes differential equations in both the forward [Eqs. (1-6)] and backward [Eq. (14)] directions. Such TPBVP is too complex for real-time operational implementation with available numerical TPBVP-solver and near-term on-line computer technology. The next two subsections describe a time-scale separation of the problem and the consequent simplification of the solution based on singular-perturbation conditions.

C. Time-Scale Separation Based on Midcourse Characteristics

The time-constants associated with the state variables are assessed by scaling the state Eqs. (1-6) with appropriate terms such that the right-hand-side expressions are nondimensional and of unit order, and the expressions on the left-hand side would represent the equation dynamics. The resulting equations appear as follows

$$\frac{r}{V}\frac{\mathrm{d}(x/r)}{\mathrm{d}t}=\cos\gamma\cos\phi \tag{15}$$

$$\frac{r}{V}\frac{\mathrm{d}(y/r)}{\mathrm{d}t}=\cos\gamma\cos\phi \tag{16}$$

$$\frac{h_{\max}}{V}\frac{\mathrm{d}(h/h_{\max})}{\mathrm{d}t}=\sin\gamma \tag{17}$$

$$\frac{V}{g}\left(\frac{1}{E}\frac{\mathrm{d}E}{\mathrm{d}t}\right)=\frac{2}{1+2gh/V^2}\frac{(T-D)}{mg} \tag{18}$$

$$\frac{mV}{L_{\max}}\frac{\mathrm{d}\phi}{\mathrm{d}t}=\frac{L}{L_{\max}}\frac{\sin\sigma}{\cos\gamma} \tag{19}$$

$$\frac{mV}{L_{\max}}\frac{\mathrm{d}\gamma}{\mathrm{d}t}=\frac{L}{L_{\max}}\cos\sigma+\frac{mg\cos\gamma}{L_{\max}} \tag{20}$$

where r represents a characteristic range for the particular scenario under consideration; $h_{\max}$ is the operational altitude limit; and $L_{\max}$ the lift limit.

Table 1 contains some typical midcourse values of BVR-missile parameters, and Table 2 shows the value of the time constants estimated from Eqs. (15-20) using the parameter values given in Table 1. Table 2 also includes the range of the autopilot/actuator time constants for a generic BVR missile, within which the values are observed to be much smaller than those of the state variables discussed above. The values in Table 2 show a clear separation in time scales associated with various components of the missile dynamics, which can be conveniently divided into four groups: 1) slowest: position components x and y, and specific energy E; 2) slow: altitude h; 3) fast: flight-path angle γ and heading angle ϕ; and 4) very fast: autopilot/actuator states. Observe that the distribution of time scales is different from that realized for the end-game problem.

D. Simplified Midcourse Guidance Solution

In this subsection, we present our approach in simplifying the optimal-guidance problem, based on singular-perturbation considerations which are justified with the time-scale separation established above. The resulting solution is near optimal and is sufficiently simple for possible real-time onboard implementation. The desired lift parameters are determined by studying the guidance problem in the various time scales but the fastest one, as the guidance law is not intended to control the autopilot/actuator dynamics.

Slowest Time Scale

The slowest variables are x, y, and E. Since h, ϕ and γ are faster, their corresponding equations may be considered to be in equilibrium in the slowest time frame. The variables are denoted in the slowest time scale by the subscript 1. The equilibrium conditions of h, ϕ, and γ imply that

$$\gamma_1=\sigma_1=0 \tag{21}$$

$$L_1=mg \tag{22}$$

and the Hamiltonian [Eq. (13)] simplifies to

$$H_1=\lambda_{x_1}V_1\cos\phi_1+\lambda_{y_1}V_1\sin\phi_1+\lambda_{E_1}\frac{V_1(T-D_1)}{mg}+1 \tag{23}$$

In this time frame, h and ϕ behave as control variables. The optimal value of ϕ is given by $\partial H_1/\partial\phi=0$, therefore,

$$\tan\phi_1=\lambda_{y_1}/\lambda_{x_1} \tag{24}$$

and ϕ_1 is constant since λ_{x_1} and λ_{y_1} are constant. From Eqs. (1), (2), and (12),

$$\phi_1=\tan^{-1}[(y_f-y_0)/(x_f-x_0)] \tag{25}$$

i.e., the flight path direction in the horizontal plane is determined by the horizontal projection of the line which joins the current missile position to the intended final missile position. Observe that Eq. (24) and the condition for free final time, $H_1(t_f)=0$, together determine λ_{x_1} and λ_{y_1}

$$\lambda_{x_1}=-\cos\phi_1/V_1(t_f) \tag{26}$$

$$\lambda_{y_1}=-\sin\phi_1/V_1(t_f) \tag{27}$$

The optimality condition of h_1 depends on λ_{E_1}. To obtain a solution of λ_{E_1} without solving the backward differential equation, the values of T and m are approximated by their average values. This removes the time-dependencies of H_1, thus an additional condition is obtained

$$H_1=\lambda_{x_1}V_1\cos\phi_1+\lambda_{y_1}V_1\sin\phi_1 + [\lambda_{E_1}V_1(T_{av}-D_1)/m_{av}g]+1=0 \tag{28}$$

Equation (28) compared to its own value at t_f gives a solution for λ_{E_1}

$$\lambda_{E_1}=\frac{m_{av}g}{(T_{av}-D_1)}\left(\frac{1}{V_1(t_f)}-\frac{1}{V_1}\right) \tag{29}$$

The optimal altitude is given by $\partial H_1/\partial h=0$, which, after elimination of the Lagrange variables through Eqs. (26), (27) and (29), becomes

$$\frac{g}{V_1^2}(T_{av}-D_1)=\left(\frac{1}{V_1(t_f)}-\frac{1}{V_1}\right)V_1\frac{\partial D_1}{\partial h} \tag{30}$$

This equation determines the optimal altitude h implicitly through the term $\partial D_1/\partial h$.

Table 2 Time constants associated with various states during midcourse

	Components	Time constant	Values, s
Position	x	r/V	100
	y	r/V	100
	h	$h_{\max}/V$	20
Velocity	Specific energy	V/g	100
	Flight path angles	$mV/L_{\max}$	2.5
Acceleration	L	Autopilot/actuator time constants	0.6 to 0.05

In view of the previous comment that the guidance law is updated at every sample instant, the approximation of T and m by T_{av} and m_{av} would affect the guidance law only during the motor burning period, which is only a small fraction of the total flight time. The intent of such approximation during this period is to summarize the effect of motor burning by the two constant quantities.

Slow Time Scale

The slow time scale is defined by the altitude dynamics which are faster than the dynamics of x, y and E, but slower than the flight path or autopilot/actuator dynamics. To solve for the altitude dynamics, λ_{x_1}, λ_{y_1}, and λ_{E_1} from the slowest time frame are used. Since flight path angle dynamics are still faster than altitude dynamics, ϕ and γ are approximated by their equilibrium state. The corresponding Hamiltonian can be written as

$$H_2 = \lambda_{x_1} V_2 \cos\gamma_2 \cos\phi_1 + \lambda_{y_1} V_2 \cos\gamma_2 \sin\phi_1 + \lambda_{h_2} V_2 \sin\gamma_2 + \lambda_{E_1} V_2 (T - D_2)/(mg) + 1 \tag{31}$$

where the subscript 2 denotes variables in the slow time scale.

The optimality condition $\partial H_2/\partial\gamma = 0$ reduces to

$$\tan\gamma_2 = \lambda_{h_2}/(\lambda_{x_1}\cos\phi_1 + \lambda_{y_1}\sin\phi_1) \tag{32}$$

To avoid solving the backward differential equation for λ_{h_2}, T and m are again approximated by their average values to give the additional condition $H_2(t) = 0$. This condition, with the Lagrange variables eliminated by Eqs. (26), (27), (29), and (32), gives

$$\frac{\sec\gamma_2 - 1}{V_1(t_f)} = \frac{V_1 - V_2}{V_1 V_2} + \frac{(D_1 - D_2)g}{V_1^3 \partial D_1/\partial h} \tag{33}$$

This equation gives a value of $\sec\gamma_2$. γ_2 is positive if $h_2 < h_1$ and is negative if $h_1 < h_2$. Note that if this equation solves out to a negative value of $(\sec\gamma_2 - 1)$, the desired flight path angle is ± 90 deg (this happens because Eq. (32) must be modified when optimal γ_2 is 90 deg.)

Now, given the current flight path angles ϕ and γ, and the desired flight path angles ϕ_1 and γ_2, the orientations of the current velocity vector and the desired velocity vector are respectively specified by

$$v_c = [\cos\gamma\cos\phi,\ \cos\gamma\sin\phi,\ \sin\gamma] \tag{34}$$

$$v_d = [\cos\gamma_2\cos\phi_1,\ \cos\gamma_2\sin\phi_1,\ \sin\gamma_2] \tag{35}$$

The lift vector net of gravity must be perpendicular to v_c and, assuming that the missile flight path dynamics is identical in all directions, then the optimal lift vector would also lie in the plane containing v_c and v_d. This defines the orientation σ, thus simplifying the solution further by removing it from the fast time scale below. Furthermore, the total angle through which the flight path must be changed is given by the dot-product relationship

$$\Delta\psi = \cos^{-1}(v_c \cdot v_d) \tag{36}$$

Fast Time Scale

The dynamics of the heading angle ϕ and flight path angle γ define the fast time scale. The Hamiltonian, with the Lagrange multipliers derived from the slower time frames, can be written as

$$H_3 = \lambda_{x_1} V_2 \cos\gamma_3 \cos\phi_3 + \lambda_{y_1} V_2 \cos\gamma_3 \sin\phi_3 + \lambda_{h_2} V_2 \sin\gamma_3 + \lambda_{E_1} V_2 \frac{(T - D_3)}{mg} + \lambda_{\phi_3} \frac{L_3 \sin\sigma_3}{mV_2 \cos\gamma_3} + \lambda_{\gamma_3} \frac{(L_3\cos\sigma_3 - mg\cos\gamma_3)}{mV_2} + 1 \tag{37}$$

The optimality conditions $\partial H_3/\partial L = 0$ and $\partial H_3/\partial\sigma = 0$ can be used to determine λ_{γ_3} and λ_{ϕ_3} in terms of L_3 and σ_3. Approximation of T and m by their average values again gives an additional condition $H_3(t) = 0$. This condition, after elimination of the Lagrange variables and the drag terms [Eqs. (7-10)], can be used to define the optimal lift L_3. Further simplifications obtained by assuming the angles $(\phi_3 - \phi_1)$ and $(\gamma_3 - \gamma_2)$ to be small, and by ignoring negligible terms, lead to

$$L_3^2 \approx -\frac{QsC_{L_\alpha}^2}{C_{D_{\alpha^2}}} \frac{V_1(T_{av} - D_1)}{2[V_1 - V_1(t_f)]} (\Delta\psi)^2 \tag{38}$$

in addition to a weight compensation term. This indicates that the optimal lift L_3 is almost proportional to $\Delta\psi$.

E. Midcourse Guidance Algorithm

A midcourse guidance algorithm can be formulated based on the results derived in Sec. IID to involve the following computations:

Slowest time scale: Heading angle ϕ_1, Eq. (25); $\partial D_1/\partial h$ and hence optimal altitude h_1, Eq. (30):

Slow time scale: Flight-path angle γ_2, Eq. (33); lift orientation σ and angle to turn $\Delta\psi$, Eqs. (34-36).

Fast time scale: Lift magnitude L_3, Eq. (38).

Calculation of ϕ_1 is straightforward. It involves the inertial angle of the straight line joining the missile position and the predicted intercept position, as projected on the horizontal plane. As explained in Sec. IIA, available missile state and target information are used to provide the intercept-position prediction, which is treated as a final condition by the formulation. It is the function of the feedback guidance to react and adapt to any perturbation in the target state that would likely exist in the future. It should be noted that the alternative missile model of using relative-position components in the horizontal plane has neither advantage nor disadvantage over the current model whatsoever. The two approaches are identical when constant-velocity targets are assumed; the difference lies in how the missile state is utilized.

The optimal altitude h_1 is defined in Eq. (30) as the value that satisfies

$$\frac{\partial D_1}{\partial h}(h_1) = \frac{g(T_{av} - D_1)V_1(t_f)}{V_1^2[V_1 - V_1(t_f)]} \tag{39}$$

where D_1 corresponds to the drag under the lift-equal-to-weight condition. There are many ways of finding the altitude h_1 that approximates this relationship. Three different methods that can be implemented real-time are described below.

If the right-hand side of Eq. (39) can be determined, then h_1 can be calculated by solving Eq. (39) as an implicit equation in h_1, with $\partial D_1/\partial h$ approximated by a finite difference. Since solving an implicit equation may violate the real-time criterion, the calculation can be sped up by solving for h_1 off-line as a function of $\partial D_1/\partial h$ and E (recall that the partial derivative of $\partial D_1/\partial h$ is determined at a fixed value of E). Hence the real-time calculation of h_1 simplifies to evaluating the right-hand side of Eq. (39) to obtain the optimal value of $\partial D_1/\partial h$, and using the resulting value and current specific energy to obtain the value of h_1 by interpolating the optimal altitude data obtained off-line.

On the other hand, it is readily observed that the right-hand side of Eq. (39) in fact depends on the optimal altitude h_1 through V_1, D_1, and $V_1(t_f)$. If h_1 is known, then V_1 can be determined by conservation of energy, D_1 can be computed as lift-equal-to-weight drag, and $V_1(t_f)$ can be estimated moderately accurately using the range-to-go. This again brings Eq. (39) back to an implcit equation in h_1. The first method for determining h_1 real-time makes use of a recursive com-

putation of h_1: an initial value of h_1 is selected to determine the right-hand side of Eq. (39), the resulting value is used to update h_1 by the table look-up method described above.

The second method makes use of a simplifcation of the right-hand-side expression of Eq. (39),

$$\dot{V}_1 \approx \frac{T_{av}-D_1}{m_{av}} \approx \frac{V_1(t_f)-V_1}{t_{go}} \tag{40}$$

This approximation brings in the need for a time-to-go estimate, even when the original problem assumes free final time. Based on this approximation, Eq. (39) becomes

$$\frac{\partial D_1}{\partial h}(h_1) \approx -\frac{m_{av}gV_1(t_f)}{V_1^2 t_{go}} \approx -\frac{m_{av}g}{V_1 t_{go}} \tag{41}$$

where the last approximation eliminates the computation of $V_1(t_f)$ without justification. This approach still requires an initial guess of h_1 or V_1, which have to be updated recursively. The software used to generate the results in this paper is based on this approach.

The third method is based on the observation that, in the absence of propulsion, the optimal altitude as a control variable in the outer solution is completely defined by the initial conditions of x, y and E, and the final condition of Eq. (11). Since the outer solution of heading angle ϕ_1 is constant as defined in Eq. (25), the optimal altitude after motor burn is completely determined by the initial horizontal range to intercept and specific energy. Any or combinations of the above methods can be used to create optimal altitude data as a function of horizontal range to intercept and specific energy. Since the motor burn time is but a small fraction of the total flight time, the same optimal altitude data can be used through this period without much penalty on performance.

Since the optimal altitude from the outer solution does not satisfy the boundary condition imposed in Eq. (11), some ad hoc correction that adjusts the optimal altitude to let it converge to the predicted intercept altitude as horizontal range decreases may improve performance. Although such altitude correction scheme has not been employed to obtain the performance evaluation in this paper, an exponential correction scheme has demonstrated improved performance under most situations in subsequent efforts to improve this guidance law.[13]

With the value of V_1 updated at the optimal altitude h_1, Eq. (33) can be solved for the optimal final path angle γ_2 explicitly. Here V_2 and D_2 are the current missile speed and drag. If

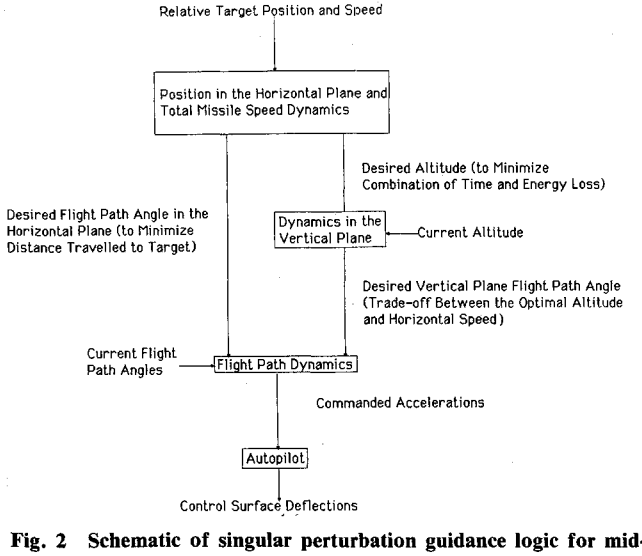

Fig. 2 Schematic of singular perturbation guidance logic for midcourse phase.

the approximation in Eq. (41) has been used to determine h_1, the same approximation can be applied to simplify Eq. (33) by further eliminating $V_1(t_f)$, leading to

$$\gamma_2 = \sec^{-1}\left[\frac{V_1}{V_2} - \frac{(D_1-D_2)t_{go}}{V_1 m_{av}}\right] \tag{42}$$

Similar to the optimal altitude calculation, an ad hoc boundary-layer correction can be devised for flight path angle γ_2 to allow it to converge to a collision-course flight path as it approaches the seeker lock-on range (see Step 3 of the algorithm below).

With the optimal flight path angle γ_2 and heading angle ϕ_1, the optimal lift orientation σ and magnitude L can be determined by Eqs. (34-36), and (38).

These engineering approximations lead to the following midcourse guidance algorithm (Fig. 2):

Given: predicted intercept location and time; and mass and thrust information, including average values.

Step 1: Determine optimal heading angle

$$\phi_1 = -\tan^{-1}(y_f-y_0)/(x_f-x_0)$$

Step 2: Determine optimal altitude h_1^* according to

$$\left.\frac{\partial D}{\partial h}\right|_E (h_1^*) = -\frac{m_{av}g}{V_1 t_{go}}$$

where V_1 is determined iteratively as shown below.

Ad-hoc boundary-layer correction on optimal altitude:

$$h_1 = h_1^*(1-e^{-k_h R}) + e^{-k_h R}h_f$$

where R = horizontal range to predicted final location; k_f = selected constant >0. (Note: This step is recommended, but was not used in obtaining the evaluation results included in this paper.)

Determine (iterate) V_1 based on

$$V_1 = \sqrt{2g[h+(V^2/2g)-h_1]}$$

Compute drag D_1 at h_1, V_1 with lift = weight.

Step 3: Determine optimal flight-path angle

$$\gamma_2^* = \sec^{-1}\left[\frac{V_1}{V} - \frac{(D_1-D)t_{go}}{V_1 m_{av}}\right]$$

Ad-hoc flight-path angle correction to assure target acquisition at seeker lock-on range:

$$\gamma_2 = k_\gamma \gamma_2^* + (1-k_\gamma)\gamma_1$$

where γ_1 = flight-path angle determined by straight line to predicted final location; $k_\gamma \in [0, 1]$ is determined according to $k_\gamma = 1$ when horizontal range to target ≥ 30 km, $k_\gamma = 0$ when slant range ≤ 10 km (assumed seeker lock-on range); and k_γ decreases linearly with range in between these two locations.

Step 4: Determine lift orientation σ by comparing desired heading and flight-path angles to current angle values.

Step 5: Determine lift acceleration magnitude

$$L/m = \sqrt{sC_{L_\alpha}^2/2m_{av}C_{D_{\alpha^2}}}\ \sqrt{QV/t_{go}}$$

Step 6: Add gravity compensation to lift vector and transform to body coordinates.

F. Mechanization Feasibility

A major requirement of the midcourse guidance algorithm is that it be feasible for real-time implementation onboard a tactical weapon with available microprocessor components. We have achieved this requirement by simplifying the optimal

guidance problem to a manageable size through singular-perturbation considerations and engineering approximations. An important step was to replace the implicit optimal altitude calculation by table look-up which can be stored in readily available read-only memory (ROM). Further simplification of the guidance law is still possible, as explained in the last subsection.

Microprocessors with 32-bit floating point capability are desirable for implementing the advanced midcourse guidance. Viable candidates that satisfy military standards are Intel's M8087 Numeric Data Processor and Fairchild's F9450. Intel's M8087 is the military version of the iAPX 86/20 microprocessor (8086-8087 combination), and CMOS versions of Fairchild's F9450 are being pursued by other manufacturers. Both processors need only a single 5 V power supply.

The main ROM requirement is that of the optimal altitude table, which, as implemented in our current missile simulation, uses 40×80 4-byte words, amounting to 12.5 K-Bytes. Only a modest amount of random-access read/write memory (RAM) would be needed to store intermediate data.

III. Simulation Examples

The guidance law obtained through application of singular-perturbation techniques on the optimal-control problem is tested using a beyond-visual-range (BVR) missile simulation.[12] The simulation uses a six-degree-of-freedom (6-DOF) mathematical model of a generic BVR tactical air-to-air missile.

Section IIIA describes the pseudo-intelligent 3-DOF target model of the simulation, which allows meaningful evaluation of the guidance's performance under air-threat situations. In Sec. IIIB two flyout examples are examined that compare the behavior of the singular-perturbation (SP) guidance law with that of a linear-optimal guidance law and a pronav guidance law. Both are provided by the sponsor as a baseline for fair evaluation. In Sec. IIIC some outer launch boundaries obtained with these guidance laws are compared.

A. Evasive Target Maneuver Algorithm

The target evasive maneuver algorithm used in the simulations was developed to satisfy a need for an effective algorithm to be used to evaluate advanced missile guidance and estimation techniques. The algorithm is designed to stress the missile engagement and not to simulate a particular target tactic employed by present-day aircraft. However, to remain within the realm of realism, certain restrictions have been placed on the maneuver algorithm such as a final-maneuver activation range and target acceleration limits.

The mechanization of this algorithm assumes that the target flies at constant speed, and has constant normal acceleration. It can instantaneously change its acceleration magnitude and orient its normal acceleration vector in any direction defined by its roll angle.

The target maneuver algorithm consists of three phases. Phase 1 commences at missile launch for ranges greater than 6,000 ft. The target performs a constant initial low-g maneuver in the yaw direction. The sign of the acceleration changes every 10 s. The maneuver starts in the positive yaw direction.

Phase 2 begins when the range has decreased to 6,000 ft. The target pulls a maximum-g maneuver in a 45-deg plane. The sign defining the plane and the sign of the maneuver acceleration in that plane both depend on the aspect angle in yaw at 6,000-ft range. Let AAY denote this angle. The target roll angle which defines the orientation of the target normal acceleration is given by

$$\left[\frac{\pi}{2}+\frac{\pi}{4}\cdot\mathrm{sgn}(\cos AAY)\right]\cdot\mathrm{sgn}(\sin AAY)$$

Phase 3 begins when the estimated time-to-go reaches 1 s. The time-to-go is estimated as range/range rate. Phase 3 commands a maximum-g maneuver straight down (i.e., the target roll angle equals π).

Table 3 Launch engagement information for performance evaluation

Missile launch altitude, m	3,048.0
Missile launch Mach	0.9
Initial target altitude, m	3,048.0
Constant target Mach	0.9
Initial target maneuver (for range greater than 6000 ft), g	2.0
Final target maneuver (for range less than 6000 ft), g	9.0
Initial off-boresight angle, deg	0
Minimum launch range, m	304.8
Miss distance requirement, m	3.0

B. Flyout Example

This subsection illustrates the behaviors of the modern guidance laws, a linear-quadratic BVR guidance, and proportional navigation with the results from sample flyout simulations. The latter two guidance schemes have preprogrammed g-bias commands during midcourse as a function of flight time to allow the missile to loft to higher altitudes where air drag is reduced. The g-bias schedule was provided by the sponsoring office.

The near-optimal guidance law based on singular perturbation (SP) simplifications, derived in Sec. II, was formulated to optimize midcourse performance. To achieve a fair evaluation

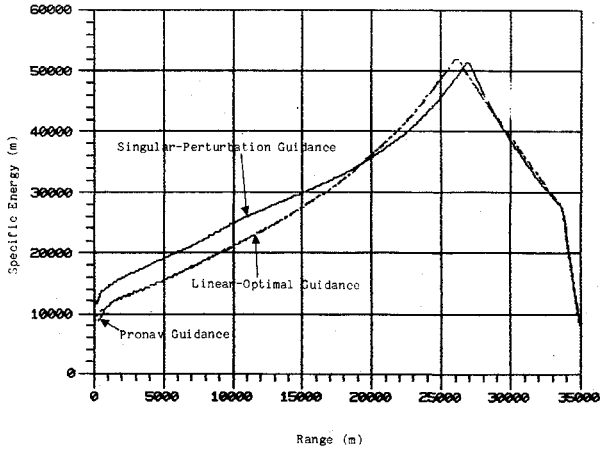

Fig. 3 Specific energy profiles.

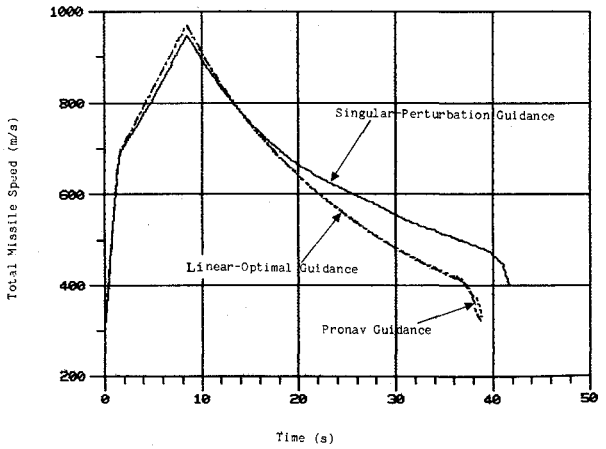

Fig. 4 Total missile speed profiles.

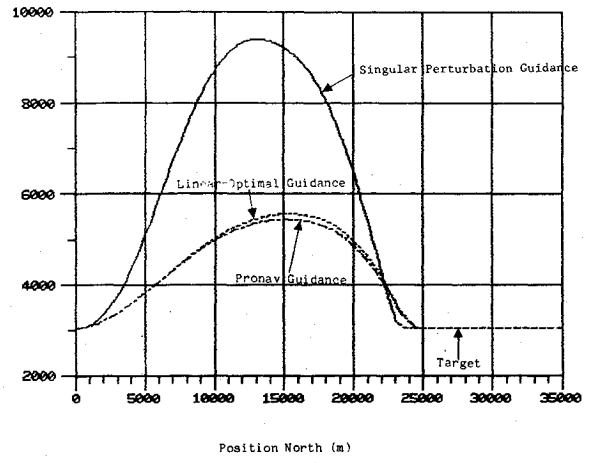

Fig. 5 Altitude profiles.

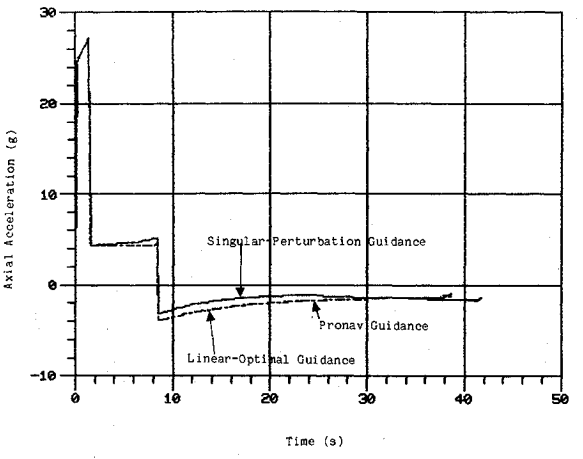

Fig. 7 Axial acceleration profiles.

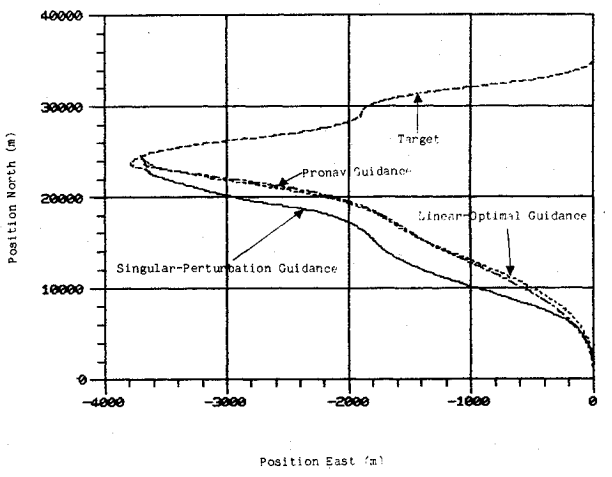

Fig. 6 Horizontal trajectories.

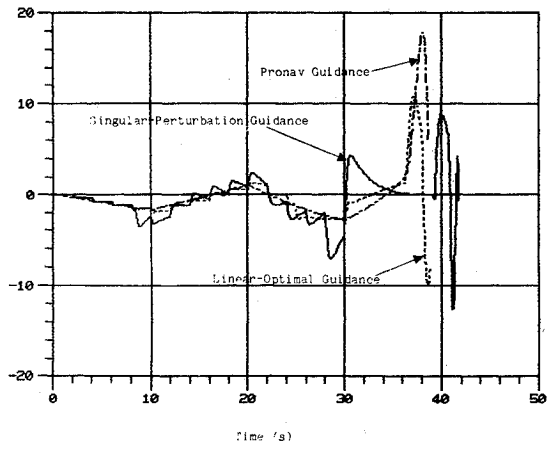

Fig. 8 Lateral acceleration profiles.

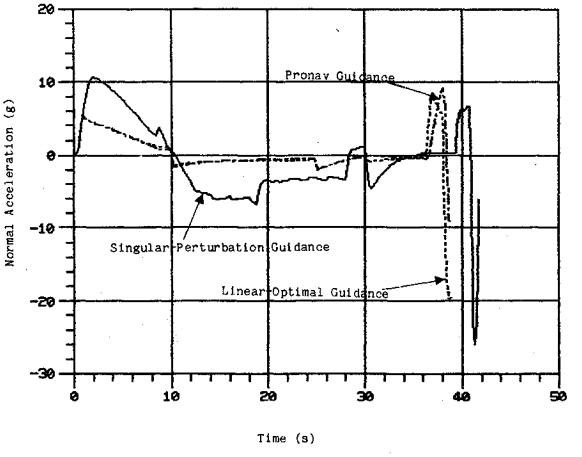

Fig. 9 Normal acceleration profiles.

of the midcourse performance between the various guidance laws, the optimal altitude of the SP guidance is ignored during terminal phase, and the linear-optimal BVR guidance is used when the range from target decreases below 2000 m. Any superiority in performance of a guidance would be a direct result of its energy-saving midcourse trajectory and ability to hand over to terminal guidance with desirable flight conditions.

The flyout example considered here compares pertinent variables of individual flyouts from all of the three guidance laws. The example is a coalitude head-on launch at 10,000 ft, with engagement conditions described by Table 3, and a launch range of 35 km. These engagement conditions are typical of those found in a fighter engagement scenario. This example compares the results from testing the singular perturbation (SP) guidance developed in Sec. II, the linear-optimal guidance, and the proportional navigation (pronav) guidance.

Results of the example are displayed in Figs. 3 to 10. Figure 3 compares the missile specific energy of the three guidance laws vs range to target. It clearly demonstrates the SP guidance's effect in preserving energy for final approach. Figures 4 and 5 illustrate the two component terms of the missile specific energy: total missile speed in Fig. 4 and altitude in Fig. 5. Figure 5 shows that the SP guidance law allows the missile to climb to an optimal altitude where drag is reduced. This results in higher terminal speed as demonstrated in Fig. 4. Although it is not obvious in Fig. 5 whether the guidance laws have scored a hit, final statistics show that the linear optimal guidance law misses the target by over 22 m, the pronav by 30 m, and the SP guidance brings the missile to within 2 m from the target, which is less than the 3-m miss-distance requirement. Figure 6 compares the horizontal trajectories of the missile driven by the three guidance laws. It is observed here that the target performs a final intelligent maneuver into the missile. Note the different scales on the two axes. Figure 7 indicates that the missile using SP guidance does experience less drag than when the other two guidances are used. Figures 8 and 9 compare the missile lateral and normal accelerations caused by the three guidance laws. Figure 10 compares their total-angle-of-attack histories.

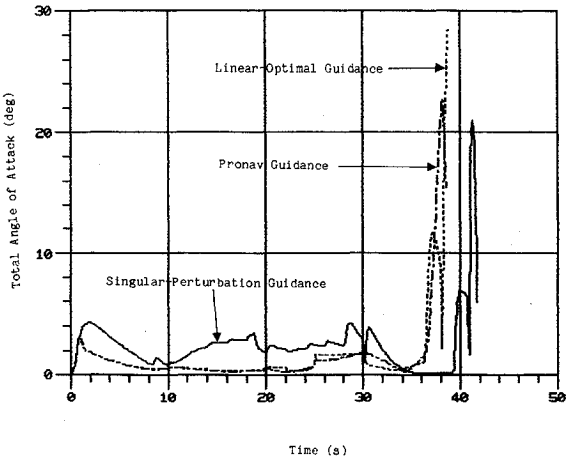

Fig. 10 Total angle of attack profiles.

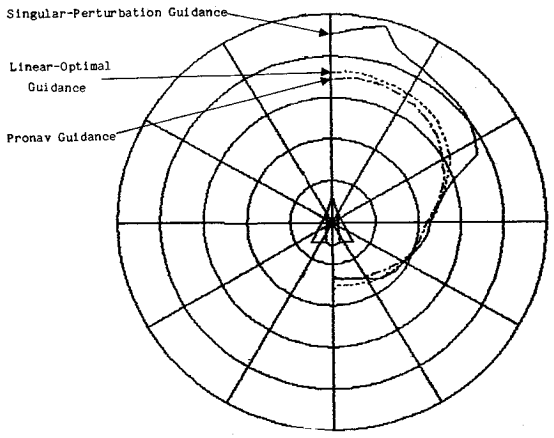

Fig. 11 Outer launch boundaries.

C. Outer Launch Boundary

Figure 11 contains the outer launch boundaries for the launch conditions in Table 3. Since the SP guidance actually uses the linear optimal guidance over the final 2000 m range as described above, the launch boundaries reflect the performance comparison due to the midcourse flight.

BVR missiles are most likely used in a head-on approach mission. From the coaltitude engagement results depicted in Fig. 11, the SP guidance law achieves almost 25 percent advantage in effective launch range over both the linear-optimal guidance law and the pronav guidance in the head-on approach. Considerable improvement is maintained for the forward quadrant of the target, but decreases to inconsequential amounts in the rearward quadrant.

IV. Conclusions

We have established an advanced midcourse guidance law for air-to-air beyond-visual-range missiles. The guidance law is obtained from the application of singular-perturbation methodologies to an optimal control formulation. The three major components of the guidance law are: 1) determine an optimal altitude for the missile, 2) compute the desired flight path angles, and 3) obtain the necessary lift command.

The advanced singular-perturbation guidance law has been evaluated against two other guidance laws provided by the sponsoring office as baseline for comparison via computer simulations. It is observed that the singular-perturbation guidance law results in increased effective launch ranges compared to the linear-optimal guidance and the pronav guidance laws. This increase is a result of the singular-perturbation midcourse guidance's minimum-time formulation. The formulation, under the singular-perturbation approximations, causes the missile to climb to an optimal altitude of lower drag to minimize its constant-altitude flight time. The resulting path also allows the missile to conserve energy for final interception of the target.

The near-optimal singular-perturbation guidance law is sufficiently simple that it is feasible for real-time and onboard implementation in air-to-air missiles with currently available microprocessor technologies. Computation can be sped up by substituting some of the complex calculations with solutions obtained off-line and stored as look-up tables in readily available read-only memories. An example of such look-up tables is the determination of optimal altitude as a function of other easily obtained parameter values in the formulation. The optimal altitude table is, in fact, actually used in the simulations.

The simplified optimal guidance formulation has also been applied successfully in the development of a real-time on-line ignition control algorithm for medium-range missiles equipped with solid-propellant variable-delay pulse motors.[13]

The near-optimality issue of the advanced midcourse guidance law is being investigated by comparing its performance to numerical optimization results, which will be the subject for future presentation.

Acknowledgment

This work was supported by the Air Force Armament Laboratory, Armament Division, Eglin AFB, Florida under Contract F08635-81-C0189.

References

[1]Sridhar, B. and Gupta, N.K., "Missile Guidance Laws Based on Singular Perturbation Methodology," *Journal of Guidance and Control,* Vol. 3, April 1980, pp. 158-165.

[2]Sridhar, B. and Gupta, N.K., "Accurate Real-Time SRAAM Guidance Using Singular Perturbation Optimal Control," *NAECON Proceedings,* May 1979, pp. 772-779.

[3]Asher, B.H., "Derivation of Proportional Guidance by Use of Optimal Control Theory," Air Force Avionics Laboratory, Wright-Patterson AFB, OH, AFAL/NVE-1-TM-73-2, 1973.

[4]Cottrell, R.G., "Optimal Intercept Guidance Laws for Short-Range Tactical Missiles," *AIAA Journal,* Vol. 9, July 1971, pp. 1414-1415.

[5]Cottrell, R.G., "Optimal and Suboptimal Guidance Laws for Air-to-Air Interception," Hughes Aircraft, IDC 2342.0520/114, Culver City, CA, Nov. 1967.

[6]Asher, R.B. and Matuszewski, J.P., "Optimal Guidance with Maneuverable Targets," *Journal of Spacecraft and Rockets,* Vol. 11, March 1974, pp. 204-206.

[7]Asher, R.B. and Matuszewski, J.P., "Optimal Guidance with Maneuverable Targets,"*Joint Automatic Control Conference,* June 1974, pp. 4-10.

[8]Bryson, A.E. and Ho, Y.C., *Applied Optimal Control,* Blaisdell, Waltham, MA, 1969.

[9]Kelley, H.J., "Aircraft Maneuver Optimization by Reduced Order Approximation," *Control and Dynamic Systems,* Vol. 10, ed. C.T. Leondes, Academic Press, New York, 1973, pp. 131-178.

[10]Calise, A.J., "Singular Perturbation Techniques for On-Line Optimal Flight Path Control," *Journal of Guidance and Control,* Vol. 4, July-Aug. 1981, pp. 398-405.

[11]Price, D.B., Calise, A.J., and Moerder, D.D., "Piloted Simulation of an Onboard Trajectory Optimization Algorithm," *Journal of Guidance, Control, and Dynamics,* Vol. 7, May-June 1984, pp. 355-360.

[12]"Six-Degree-of-Freedom Mathematical Model for a Generic Beyond-Visual-Range Missile," prepared for AFATL/DLMA by the General Research Corporation under Contract DASG60-80-0009, CLIN0004, AFATL/DLMA, Eglin AFB, FL, June 1981.

[13]Cheng, V.H.L., Menon, P.K.A., Gupta, N.K., and Briggs, M.M., "A Reduced-Order Approach to Near-Optimal Real-Time Pulse-Motor Ignition Control," AIAA Paper 85-0500, Jan. 1985.